Tensor Study of Quantum Link Model

P. Stornati, P. Krah, D. Banerjee

Date: April 9, 2020

---

1 Hamiltonian of QLM as a spin system

We want to study the Square Ice Hamiltonian

$$\mathcal{H} = \sum_{\square} (-f_{\square} + \lambda f_{\square}^2)\,, \tag{1}$$

as the sum over all plaquettes:

$$f_{\square} = \sigma^+_{\mu_1}\sigma^+_{\mu_2}\sigma^-_{\mu_3}\sigma^-_{\mu_4} + \sigma^-_{\mu_1}\sigma^-_{\mu_2}\sigma^+_{\mu_3}\sigma^+_{\mu_4}. \tag{2}$$

on a long cylindrical lattice

$$\Omega = \{\mu = (n,m) |\, n \in \{1,\dots,L_x\},\ m \in \{1,\dots L_y\}\} \tag{3}$$

displayed in fig. 1.

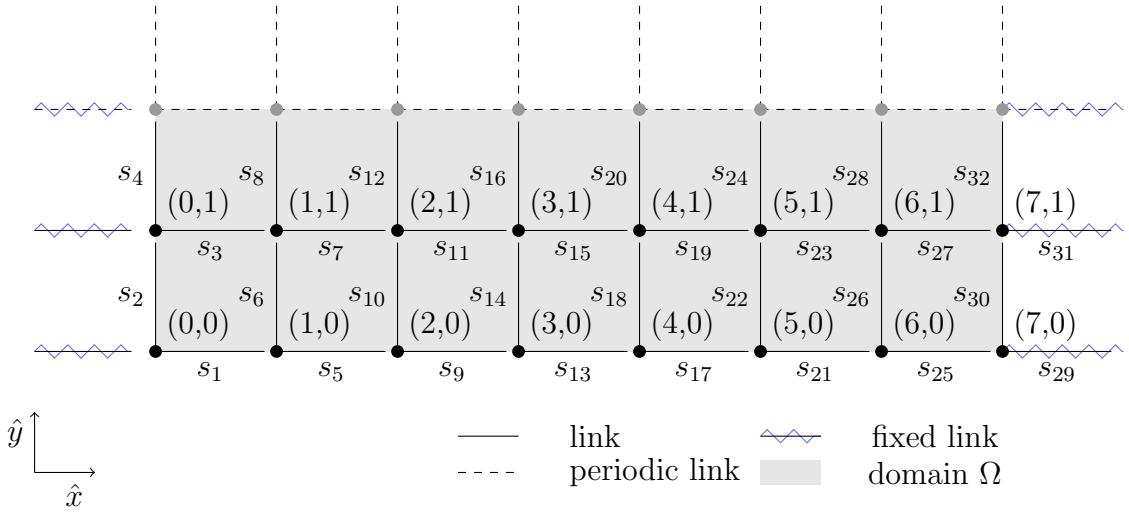

Figure 1: Definition of the computational mesh

In the conventional up/down $s^{\pm} \in \mathbb{R}^2$ ([1 0]/[0 1]) basis the link operators $\sigma^{\pm}$ are pauli matrices :

$$\sigma^+ = \begin{pmatrix} 0 & 1 \\ 0 & 0 \end{pmatrix} \quad \sigma^- = \begin{pmatrix} 0 & 0 \\ 1 & 0 \end{pmatrix} \qquad I_2 = \begin{pmatrix} 1 & 0 \\ 0 & 1 \end{pmatrix} \tag{4}$$

In all our lattices $L_y \ll L_x$. For now we fix $L_y = 2$ as in fig. 1. Before explaining the computations we want to point out some properties of the Hamiltonian.

1.1 Mathematical Properties of the Quantum Link Model

Gauss Law: The Hamiltonian $\mathcal{H}$ in eq. (1) commutes with the *vertex operator* G_μ, which counts the number of in and outgoing arrows at vertex μ. We can therefore fix the total charge at each vertex with the *Gauss law constraint*:

$$G_\mu = 0 \qquad \text{for all} \qquad \mu \in \Omega\,, \tag{5}$$

$$G_\mu := \sum_{\hat{i}\in\{\hat{x},\hat{y}\}} \left(s_{\nu-\hat{i}/2} - s_{\nu+\hat{i}/2}\right). \tag{6}$$

Winding Numbers

$$W_y = \frac{1}{2L_y}\sum_\mu E_{\mu,x} \tag{7}$$

Fluxes

1.2 Hilbert-Space

In the absence of the ice rule eq.(5) the hilbertspace becomes $2^{2\cdot L_x L_y}$ dimensional and the linear combination of every state is given by:

$$|\psi\rangle = \sum_{i_1,i_2,\ldots,i_{L_x}} A_{i_1,i_2,\ldots,i_{L_x}} |i_1\rangle|i_2\rangle\ldots|i_{L_x}\rangle \tag{8}$$

where $i_n = 1, 2, \ldots, 2^{2L_y}$ labels the corresponding quantum state at site n. For the $L_y = 2$ we thus have 16 different quantum states at each site $|i_n\rangle = |(s_1, s_2, s_3, s_4)\rangle$, where $s_i \in \{0, 1\}$ labels the ith spin in the local basis drawn in fig. 2. The 16 different combinations in the set can be explicitly written down:

$$\left\{ \begin{pmatrix}1\\1\\1\\1\end{pmatrix}, \begin{pmatrix}1\\0\\1\\1\end{pmatrix}, \begin{pmatrix}1\\1\\0\\1\end{pmatrix}, \begin{pmatrix}1\\1\\1\\0\end{pmatrix}, \begin{pmatrix}0\\0\\1\\1\end{pmatrix}, \ldots, \begin{pmatrix}0\\0\\0\\1\end{pmatrix}, \begin{pmatrix}0\\0\\0\\0\end{pmatrix} \right\} \tag{9}$$

The number of elements in the set will be also referred to as local hilbertspace dimension D.

2 Computational Basis

For the MPS we have to rewrite the Hamiltonian of the system in the nearest neighbour setting. The local Hamiltonian $H_{n,n+1}$ thus defines the interaction between the states at site $|i_n\rangle$ and $|i_{n+1}\rangle$. The Hamilton operator (1) consists of 4 terms. Where on each site we have $m = 1, \ldots, L_y$ possible interactions. Thus the hamiltonian consists of $4L_y$ Kronecker products:

$$H_{n,n+1} = \sum_{j=1}^{4} \sum_{m=1}^{L_y} h^{(j)}_{\sqsubset,n,m} \otimes h^{(j)}_{\sqsupset,n+1,m} \tag{10}$$

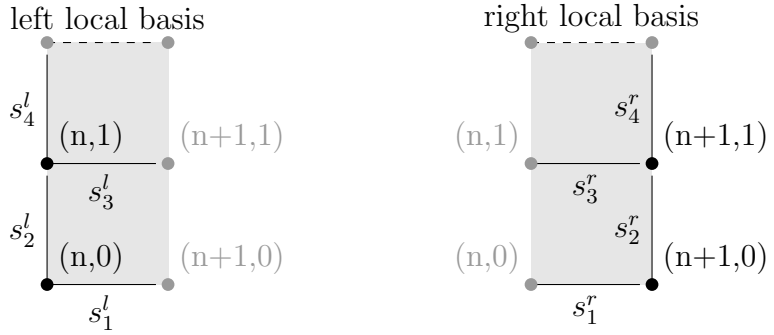

Figure 2: Definition of the computational mesh

To identify the different local interaction terms in the Hamilton operator (10) with (1) we rewrite the plaquette-operator into our computational basis $|i_n\rangle$. A plaquette operator defines our nearest neighbor interaction between state $|i_n\rangle$ and $|i_{n+1}\rangle$

$$f_{\square} = f_{\sqsubset,n,m} \otimes f_{\sqsupset,n,m} + h.c. \tag{11}$$
$$f_{\sqsubset,n,m} = \sigma^-_{r,n,m+1}\sigma^-_{v,n,m+1}\sigma^+_{r,n,m} \tag{12}$$
$$f_{\sqsupset,n+1,m} = \sigma^+_{l,n+1,m+1}\sigma^+_{v,n+1,m+1}\sigma^-_{l,n+1,m} \tag{13}$$

Comparing this to (10) yields:

$$h^{(1)}_{\sqsubset,n,m} = -f_{\sqsubset,n,m} \qquad h^{(1)}_{\sqsupset,n+1,m} = f_{\sqsupset,n+1,m} \tag{14}$$
$$h^{(2)}_{\sqsubset,n,m} = -f^\dagger_{\sqsubset,n,m} \qquad h^{(2)}_{\sqsupset,n+1,m} = f^\dagger_{\sqsupset,n+1,m} \tag{15}$$
$$h^{(3)}_{\sqsubset,n,m} = \lambda f^\dagger_{\sqsubset,n,m} f_{\sqsubset,n,m} \qquad h^{(3)}_{\sqsupset,n+1,m} = f^\dagger_{\sqsupset,n+1,m} f_{\sqsupset,n+1,m} \tag{16}$$
$$h^{(4)}_{\sqsubset,n,m} = \lambda f_{\sqsubset,n,m} f^\dagger_{\sqsubset,n,m} \qquad h^{(4)}_{\sqsupset,n+1,m} = f_{\sqsupset,n+1,m} f^\dagger_{\sqsupset,n+1,m} \tag{17}$$
$$\tag{18}$$

For example in our $L_y = 2$ system we get 64×64 size Operators :

$$h^{(1)}_{\sqsubset,n,m} = -\sigma^+ \otimes \sigma^- \otimes \sigma^+ \otimes I_2 \otimes I_2 \otimes I_2 \in \mathbb{R}^{2^6,2^6} \tag{19}$$
$$h^{(1)}_{\sqsupset,n,m} = I_2 \otimes I_2 \otimes \sigma^+ \otimes I_2 \otimes \sigma^- \otimes \sigma^+ \in \mathbb{R}^{2^6,2^6} \tag{20}$$
$$\tag{21}$$

Note that this allready inherits the periodicity in $\hat{y}$. For the choosen up/down ([1 0]/[0 1]) basis the link operators are given by:

$$\sigma^+ = \begin{pmatrix} 0 & 1 \\ 0 & 0 \end{pmatrix} \quad \sigma^- = \begin{pmatrix} 0 & 0 \\ 1 & 0 \end{pmatrix} \qquad I_2 = \begin{pmatrix} 1 & 0 \\ 0 & 1 \end{pmatrix} \tag{22}$$

$$f_{\square}^2 = \sigma_{\mu_1}^+ \sigma_{\mu_1}^- \, \sigma_{\mu_2}^+ \sigma_{\mu_2}^- \, \sigma_{\mu_3}^- \sigma_{\mu_3}^+ \, \sigma_{\mu_4}^- \sigma_{\mu_4}^+ \; + hc \tag{23}$$

If we define $p+$ and $p+$ as:

$$p+ = \frac{\mathbb{1} + \sigma^z}{2} \; ; \; p- = \frac{\mathbb{1} - \sigma^z}{2} \tag{24}$$

I have:

$$f_{\square}^2 = p_{\mu_1}^+ p_{\mu_2}^+ p_{\mu_3}^- p_{\mu_4}^- \; + p_{\mu_1}^- p_{\mu_2}^- p_{\mu_3}^+ p_{\mu_4}^+ \tag{25}$$

2.1 Todos

- Hamiltonian in external magnetic field, $\phi_{\square} \in \mathbb{R}$. Therefore we define the generalized plaquette operator

  $$f(\phi_{\square}) := u_{\square} e^{i\phi_{\square}} + u_{\square}^{\dagger} e^{-i\phi_{\square}} \tag{26}$$

  and plug it in (1)

- Winding number operators

  $$W_y = \tag{27}$$

3 Order Parameters

To detect the phase transitions, we study the so-called sublattice magnetization $(\mathcal{M}_{\mathrm{A}}, \mathcal{M}_{\mathrm{B}})$ which are defined as follows:

$$\mathcal{M}_{\mathrm{A}}(x) = \mathbb{P}_{x,\mu}^+ \mathbb{P}_{x+\mu,\nu}^+ \mathbb{P}_{x+\nu,\mu}^- \mathbb{P}_{x,\nu}^- - \mathbb{P}_{x,\mu}^- \mathbb{P}_{x+\mu,\nu}^- \mathbb{P}_{x+\nu,\mu}^+ \mathbb{P}_{x,\nu}^+ \tag{28}$$

where $\mathbb{P}_{x,\mu}^+$ and $\mathbb{P}_{x,\mu}^-$ are the projection operators on the spin components $S^z = \pm\frac{1}{2}$ respectively.

4 Numerical Results and Simulation Parameters

Table 1: Parameter sets for all Simulations

Parameters	Simulation 1	Simulation 2
Vertical grid size L_x	20,40,60,100,200	60
Horizontal grid size L_y	2	2
Coupling λ	$[-4.0, -3.5, -3.0, \ldots, -1.0]$	-1.0
Magnetic field angle θ	0	$\theta_k = \frac{\pi}{4}k, k = 0, 1, \ldots, 8$

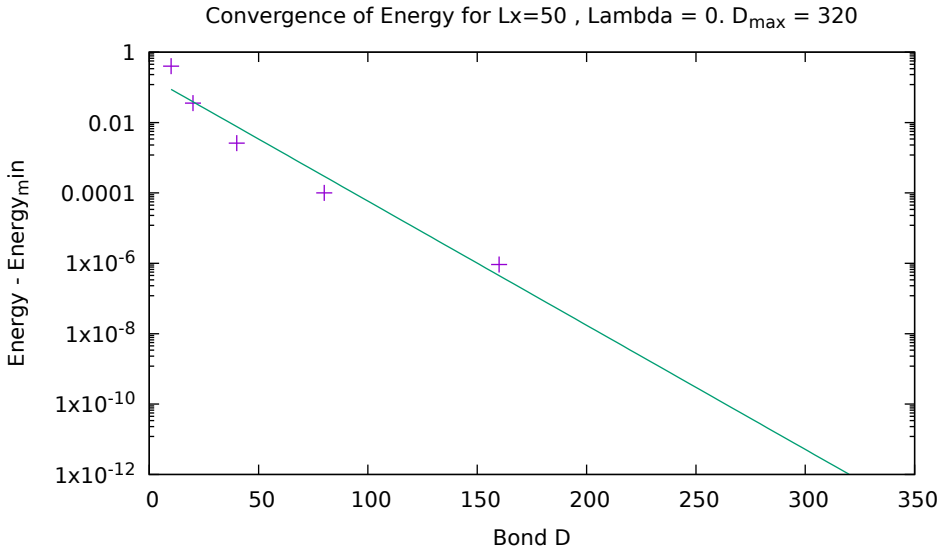

Figure 3: Extrapolation of the bond dimension